Journal of Catalysis 265 (2009) 26–34

Contents lists available at ScienceDirect

Journal of Catalysis

journal homepage: www.elsevier.com/locate/jcat

One-step synthesis of H–β zeolite-enwrapped Co/Al_2O_3 Fischer–Tropsch catalyst with high spatial selectivity

Xingang Li [a], Jingjiang He [b], Ming Meng [a], Yoshiharu Yoneyama [b], Noritatsu Tsubaki [b,c,*]

[a] Tianjin Key Laboratory of Applied Catalysis Science and Technology, School of Chemical Engineering and Technology, Tianjin University, Tianjin 300072, PR China
[b] Department of Applied Chemistry, School of Engineering, University of Toyama, Gofuku 3190, Toyama City, Toyama 930-8555, Japan
[c] JST, CREST, Sanbancho 5, Chiyoda-ku, Tokyo 102-0075, Japan

ARTICLE INFO

Article history:
Received 8 April 2009
Revised 10 April 2009
Accepted 10 April 2009
Available online 12 May 2009

Keywords:
H–β zeolite coating
Encapsulated catalyst
Core–shell structure
Fischer–Tropsch synthesis
Isoparaffin synthesis
Spatial selectivity

ABSTRACT

A tailor-made encapsulated catalyst with a H–β zeolite shell has been directly synthesized over Co/Al_2O_3 pellets to form a core–shell structure without pinholes and cracks by a hydrothermal synthesis method. Pretreatment of the Co/Al_2O_3 pellets with reflux of hot TEAOH solution can clean and corrode the pellet surface due to its strong basicity, and can enlarge the mean pore size of the pellets. Impregnation of the Co/Al_2O_3 pellets in EtOH is important to avoid the corrosion of the internal pores, to prevent the introduction of Co species into the zeolite coating, and to realize a pure and uniformed β-zeolite coating. For the catalytic reaction of direct isoparaffin synthesis from syngas, the molar ratio of $C_{isoparaffin}/C_{normal\text{-}paraffin}$ of the products obtained from the encapsulated catalyst increased about 64% than that of the products obtained from physical-mixed components. This concept of encapsulated catalyst can be useful to carry out various consecutive or multiple-step catalytic processes, where multiple reactions occur on different active centers.

1. Introduction

Because of the spatial selectivity offered by the unique pore and channel structure, zeolite membranes have been studied widely for separation. They can be supported onto inert materials, such as α-Al_2O_3, SiO_2, and stainless steel [1–4], to separate target molecules from mixtures, and can be incorporated in membrane reactors to separate products and overcome thermodynamic equilibrium limitations [5–7]. In almost all these cases, the zeolite membrane acts as an inert material without any catalytic activity.

The trapping of catalytic active species into a selective penetrable shell to form micro-encapsulated or nano-encapsulated catalysts with a core–shell structure has been reported, utilizing zeolite or carbon shells [8–15]. In most of these studies, the shell was only used for product or reactant separation. For example, the zeolite coating used was silicate-1, without acidic sites included [8,15].

On the other hand, physical-mixed catalysts with multiple functions are often used to carry out several catalytic reactions in one step in complex chemical processes. For example, Fischer–Tropsch synthesis (FTS) can produce synthetic diesel (normal paraffins) with Co-, Ru-, or Fe-based catalysts from syngas ($CO + H_2$), which can be obtained from resources such as coal, biomass, natural gas, and garbage [16]. After removing FTS by-products such as water and gaseous hydrocarbons, premier gasoline (branched paraffins) can be produced from FTS diesel in a separate reactor using solid acid catalysts, as in the Shell SMDS plant in Malaysia. It is well known that zeolites present good performance for hydrocracking and isomerization due to their acidic properties [17]. Accordingly, mixtures of H-type zeolite catalysts and FTS catalysts such as Co/SiO_2 [18,19] and iron-based catalyst [20] have been employed to produce isoparaffins directly from syngas. Long-chain normal paraffins including wax produced by the FTS catalyst are decomposed and transformed in situ to gasoline-range hydrocarbons by hydrocracking process and isomerization to isoparaffins with the aid of H_2 from syngas on the zeolite catalyst. This method can also treat FT wax, which generally deactivates FTS metallic catalysts, to form isoparaffins, the target products. It should be noted that loading of FTS active metals such as Co, Fe, or Ru directly onto zeolite supports to form metal-zeolite catalysts aiming at one-step isoparaffin synthesis from syngas is impractical because Co, Fe, or Ru on the zeolite surface cannot be easily reduced. Strong interactions between the zeolite and the precursors of these metals, generally oxides, make the extent of reduction of the supported metal quite low, resulting in a low FTS activity [21,22].

However, this kind of catalyst has no spatial relationship with component catalysts. For the physical-mixed H-ZSM-5 and Co/SiO_2 catalyst [18,19], syngas formed linear hydrocarbons on cobalt catalyst, and then these FTS hydrocarbons migrated to the

* Corresponding author. Addres: Department of Applied Chemistry, School of Engineering, University of Toyama, Gofuku 3190, Toyama City, Toyama 930-8555, Japan.
E-mail address: tsubaki@eng.u-toyama.ac.jp (N. Tsubaki).

0021-9517/$ - see front matter © 2009 Elsevier Inc. All rights reserved.
doi:10.1016/j.jcat.2009.04.009

neighboring H-ZSM-5 catalyst for hydrocracking and isomerization. Unfortunately, a part of FTS hydrocarbons desorbed directly and escaped without contact with the zeolite catalyst. This induced a high selectivity of the residual heavy FTS hydrocarbons (normal paraffins).

Due to the drawback of the hybrid catalyst, a two-stage reactor was designed, i.e. FTS catalyst in the first one, and H-type zeolite in the second one, in our previous study [23]. It was found that the distribution of carbon number of the hydrocarbons was extremely confined after the gas passed through the second reactor. To save energy and improve economic efficiency, our group firstly proposed one kind of encapsulated catalyst by coating H-ZSM-5 zeolite onto Co/SiO_2 pellet for one-step synthesis of isoparaffins from syngas [24,25]. It was found that the encapsulated H-ZSM-5/Co/SiO_2 catalyst could remove all the C_{11+} hydrocarbons, while the physical-mixed catalyst with the same composition still had a lot of C_{11}–C_{25} products. Recently, a tailor-made encapsulated catalyst, i.e. H–β zeolite shell directly enwrapped Co/Al_2O_3 FTS catalyst pellet [26] by one step, was designed through a hydrothermal synthesis process. This novel H–β/Co/Al_2O_3 encapsulated catalyst presented not only a much higher isoparaffin selectivity but also a more perfect zeolite coating formation than the previous H-ZSM-5/Co/SiO_2 encapsulated catalyst [24,25]. The conventional H–β zeolite preparation method by ion-exchange from Na-β zeolite [27–29] is not applicable to our study since Na is considered to be a poison for FTS process [30,31].

In this paper, the preparation method and synthesis mechanism are elucidated and discussed in detail. The structure of the encapsulated catalyst was characterized by X-ray diffraction (XRD), scanning electron microscope (SEM), and energy-diffusive X-ray spectroscopy (EDX) analysis, and the catalytic activity of the encapsulated catalyst for isoparaffin synthesis directly from syngas was also investigated and compared with that of the physical-mixed catalyst.

2. Experimental

2.1. Catalysts preparation

2.1.1. Preparation of Co/Al_2O_3 FTS catalyst

Co/Al_2O_3 FTS catalyst was prepared by a conventional incipient wetness impregnation method. An aqueous solution of $Co(NO_3)_2$ was added to γ-Al_2O_3 (JRC-ALO-6, JGC Universal Ltd.; specific surface area: 180 $m^2\,g^{-1}$ and pore volume: 0.93 $cm^3\,g^{-1}$) pellets, which had been heated at 400 °C for 2 h in air before the impregnation. The catalyst precursor was evaporated for 1 h, dried at 120 °C for 12 h, and was then calcined in air at 400 °C for 2 h. The size of catalyst pellet was 0.85 to 1.7 mm. The cobalt loading in the samples was 7 wt%.

2.1.2. Preparation of H–β zeolites and H–β/Co/Al_2O_3 encapsulated catalysts

For H–β zeolite precursor solution preparation, 4.1 g of SiO_2 (Aerosil 200, fumed, Silica content: 99.8%, particle: 0.014 μm, surface area: 200 $m^2\,g^{-1}$, Sigma–Aldrich, Inc.), 14.4 g of 25 wt% TEAOH in water, 0.3 g of $((CH_3)_2CHO)_3Al$ (Aluminum iso-propoxide, Sigma–Aldrich, Inc.), and 3.6 g of deionized water were mixed under continuous stirring at room temperature for 2 h. The composition of the H–β zeolite precursor solution was at a molar ratio of $96.53SiO_2$:34.55TEAOH:$1.0Al_2O_3$:$1130H_2O$.

The H–β/Co/Al_2O_3 encapsulated catalysts were prepared by a hydrothermal synthesis method. A H–β zeolite coating was directly constructed onto the pretreated Co/Al_2O_3. Three methods were used to pretreat the Co/Al_2O_3 FTS catalyst pellets before they were added into the zeolite precursor solution: (1) vacuuming for 1 h, soaking in a 25 wt% TEAOH (tetraethylammonium hydroxide) solution, treating by ultrasonication (38 W) for 15 min, followed by filtration (denoted as method T1); (2) heating under a reflux of a 25 wt% TEAOH solution at 114 °C for 4 h, followed by filtration (denoted as method T2); and (3) heating under a reflux of a 25 wt% TEAOH solution at 114 °C for 4 h, washing with distilled water thrice, and then immersing into an absolute ethanol liquid (purity > 99.5%) for 24 h, followed by filtration. This method is denoted as T3.

For the hydrothermal synthesis process, 2.0 g of pretreated Co/Al_2O_3 catalyst (pellet sizes: 0.85 to 1.7 mm) and 22.4 g of H–β zeolite precursor solution were added into a hydrothermal synthesis equipment (DRM-420DA, Hiro Company). Crystallization of the zeolite was carried out at 155 °C and at a rotation speed of 2 rpm for 3 days. The obtained catalyst was filtered from the solution and was washed with distilled water until its pH value was less than 8. It was then dried at 120 °C for 12 h and was calcined at 550 °C for 8 h in air. The synthesized catalyst, distinguished from the catalysts prepared by the different Co/Al_2O_3 pellet pretreatment methods, was denoted as H–β/Co/Al_2O_3-T1, H–β/Co/Al_2O_3-T2, or H–β/Co/Al_2O_3-T3. The weight of H–β zeolite coating on the H–β/Co/Al_2O_3-T3 catalyst was found to be 23.2 wt%.

Moreover, direct synthesis of H–β zeolite was also performed through the hydrothermal process with the same zeolite precursor solution and preparation procedure, as mentioned above, without adding Co/Al_2O_3 pellets. The crystallization temperature was 155 or 175 °C, and the crystallization time was 1, 2, or 3 days.

2.1.3. Preparation of hybrid catalyst

The mixture of Co/Al_2O_3 and H–β catalyst was prepared by mechanically mixing Co/Al_2O_3 FTS catalyst and H–β zeolite, synthesized with H–β zeolite precursor solution under the preparation condition that was the same as that used for the encapsulated catalysts. The weight of H–β zeolite was 23.1 wt%, a loading that was the same as that for the encapsulated catalyst. The obtained hybrid catalyst was denoted as H–β/Co/Al_2O_3-MX.

All the chemicals were supplied by Wako Pure Chemicals Ltd., unless indicated otherwise.

2.2. Catalysts characterization

The pore size distribution of the catalysts was obtained by N_2 physisorption using an automatic gas adsorption system (Quantachrome, Autosorb-1, Yuasa Co.) at −196 °C. The sample was outgassed at 200 °C overnight prior to N_2 physisorption.

Co dispersion of the Co/Al_2O_3 pellet catalysts prepared by the T3 pretreatment was determined by H_2 chemical adsorption with an apparatus that was the same as that used for the previous N_2 physisorption experiment. Prior to the measurement, the samples were degassed at 300 °C and at 3.0 Pa for 1 h, reduced in flowing H_2 at 400 °C for 10 h, and evacuated at 350 °C for 1 h to desorb any H_2, followed by cooling to 100 °C. The H_2 chemisorbed uptakes were measured with the double-isotherms method at 100 °C by assuming that one cobalt atom was covered by one hydrogen atom [32,33], and the dispersion percentage D% was calculated with the following equation:

$$D\% = \frac{1.179X}{Wf} \tag{1}$$

where X is the total H_2 uptake in micromoles per gram catalyst, W is the weight percentage of cobalt, and f is the fraction of cobalt reduced to the metal determined from O_2 titration.

The O_2 titration experiment was carried out at 400 °C to determine the reduction degree of the pre-reduced catalysts with the assumption that the metallic cobalt atoms oxidized totally to

Co_3O_4 [34]. The average crystal diameter in nanometers was calculated from *D*%, considering spherical metal crystallites of a uniform diameter d_p with a site density of 14.6 atoms nm^{-2}:

$$d_p = \frac{96}{D\%} \quad (2)$$

The X-ray diffraction (XRD) patterns were obtained on a RINT 2400 powder diffractometer (Rigaku Co.) in a step mode employing CuKα radiation (λ = 0.154 nm). The X-ray tube was operated at 40 kV and at 40 mA. The average Co_3O_4 particle size *d* was calculated with Sherrer formula:

$$d = \frac{0.89\lambda}{\beta \cos\theta} \quad (3)$$

where λ is the wavelength of X-ray and β is the width in radians at the half height of the Co_3O_4 [3 1 1] diffraction peak with 2θ = 36.9°.

The morphology of the samples was investigated with a JSM-6700F field emission scanning electron microscope (FE-SEM) and a scanning electron microscope (SEM) equipped with an energy-diffusive X-ray spectroscopy (EDX) attachment (JEOL JSM-6360LV), which can simultaneously provide the surface elemental composition information.

Thermal analysis was carried out with the catalysts after 10 h FTS reaction on a DTG-60 (Shimadzu) to investigate the possible coke and FTS wax which formed on the catalyst. It was implemented in an air flow of 50 ml min^{-1}. The temperature increased from 25 to 500 °C at a rate of 5 °C min^{-1}.

2.3. Fischer–Tropsch synthesis test

The FTS reaction was carried out utilizing a continuous flowing fixed-bed reactor, and an ice trap with the solvent and inner standard was equipped after the reactor to capture the heavy hydrocarbons in the effluent. The weight of catalyst was 0.5 g on the base of Co/Al_2O_3, i.e. 0.5 g of Co/Al_2O_3 FTS catalyst, 0.65 g of the H–β/Co/Al_2O_3-MX catalyst with 23.1 wt% zeolite, or 0.65 g of the H–β/Co/Al_2O_3-T3 catalyst with 23.2 wt% zeolite. Reaction conditions were 265 °C, 1.0 MPa, molar ratio of H_2/CO = 2.2, and $W_{Co/Al_2O_3}/F$ = 10 g h mol^{-1}. A detailed product analysis has been reported elsewhere [24,25]. Briefly, the effluent gas released from the reactor was analyzed by an online gas chromatograph (Shimadzu, GC-8A) using an active charcoal column equipped with a thermal conductivity detector (TCD). The products of light hydrocarbons (C_1–C_{10}) were also analyzed by an online gas chromatograph (GC-FID, Shimadzu, GC-14B) with a capillary column (J&W Scientific GS-Alumina, i.d. 0.53 mm, length = 30 m) to separate isoparaffins and normal paraffins. The products with a carbon number higher than 10 were analyzed with a high-temperature distillation-type gas chromatograph (HP-6890).

3. Results and discussion

3.1. Characterization of directly synthesized H–β zeolite

XRD patterns of the H–β zeolites synthesized with zeolite precursor solution under different crystallization temperatures and time are presented in Fig. 1. It shows that a pure β-type zeolite framework can be constructed at 155 °C and at a crystallization time that is no less than 2 days (Fig. 1a and b). It also shows that H-ZSM-5 zeolite crystalline phases will appear accompanying the H–β zeolite phases' growth at 175 °C (Fig. 1d) or at a crystallization time of less than 2 days (Fig. 1c). It indicates that the strict crystallization temperature and prolonged crystallization time are necessary to build a full H–β zeolite structure. Moreover, the peak intensity of the zeolites increases with crystallization time, indicating an increase in zeolite loading following the prolonged synthesis process.

3.2. Characterization of H–β/Co/Al_2O_3 encapsulated catalyst with a core–shell structure

XRD patterns of the H–β zeolite-coated Co/Al_2O_3 catalysts, synthesized with different Co/Al_2O_3 pellet pretreatments, are presented in Fig. 2. For the Co/Al_2O_3 catalyst (Fig. 2a), the mean Co_3O_4 particle size of 13.8 nm is determined by Scherrer formula with the Co_3O_4 [3 1 1] diffraction peak at 2θ = 36.9°, as mentioned in Experimental 2.2. As shown in Fig. 2b and c, their profiles have the similar diffraction peaks, which belongs to Co_3O_4 and Al_2O_3 phases, for both the position and intensity to that of the diffraction peaks of the Co/Al_2O_3 FTS catalyst (Fig. 2a). No β-type zeolite is coated on the Co/Al_2O_3 catalyst pellet without any Co/Al_2O_3 pellet pretreatment (Fig. 2b), and only a weak diffraction peak at 22.5°, which is ascribed to the strongest diffraction peak of β-type zeolite, is observed in the profile of the H–β/Co/Al_2O_3-T1 catalyst shown in Fig. 2c. After the hydrothermal synthesis, the mean size of the Co_3O_4 particles supported on the Al_2O_3 pellets decreases from 13.8 to 12.5 and 12.7 nm, respectively. Whereas the XRD pattern of the solid deposited in the residual hydrothermal synthesis liquid after H–β/Co/Al_2O_3-T1 preparation clearly shows that a β-type zeolite structure has been formed (Fig. 2d). It reveals that the H–β zeolite shell is very difficult to be directly coated onto the Co/Al_2O_3 catalyst pellets pretreated with the T1 method or without any pretreatment. On the other two XRD patterns of the H–β/Co/Al_2O_3-T2 and H–β/Co/Al_2O_3-T3 catalysts, three kinds of crystalline phases,

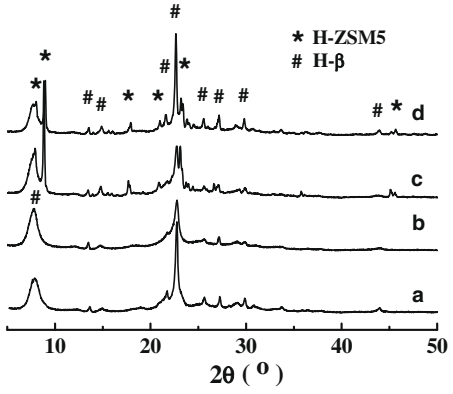

Fig. 1. XRD patterns of H–β zeolites synthesized under different crystallization conditions: (a–c) at 155 °C and (d) at 175 °C; (a) for 3 days, (b and d) for 2 days, and (c) for 1 day.

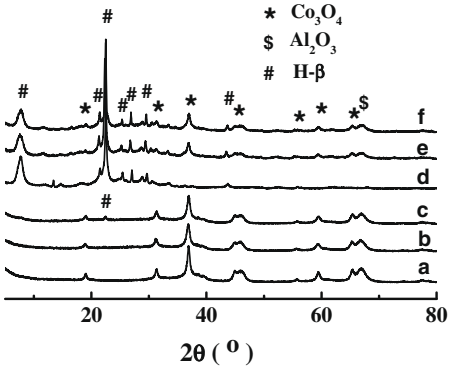

Fig. 2. XRD patterns of (a) Co/Al_2O_3 catalyst, (b) H–β/Co/Al_2O_3 without any pretreatment, (c) H–β/Co/Al_2O_3-T1 catalyst, (d) solid obtained from the residual hydrothermal synthesis liquid with T1 pretreatment, (e) H–β/Co/Al_2O_3-T2 catalyst, and (f) H–β/Co/Al_2O_3-T3 catalyst.

Table 1
The structure characteristics of the catalysts.

Catalyst	Pore volume ($cm^3\ g^{-1}$)[a]		Surface area ($m^2\ g^{-1}$)	Co_3O_4 size[b] (nm)
	Meso/Macropore	Micropore		
Al_2O_3	0.926	0.069	179.2	/
Co/Al_2O_3	0.773	0.062	167.7	13.8
H–β/Co/Al_2O_3-T3	0.435	0.108	252.5	11.8
H–β[c]	0.239	0.351	719.2	/

[a] Obtained from N_2 physisorption experiments.
[b] Calculated from XRD patterns with Scherrer formula.
[c] The precursor composition and hydrothermal synthesis condition are the same as those for the H–β/Co/Al_2O_3-T3 catalyst.

i.e. the H–β zeolite, Co_3O_4, and Al_2O_3, are observed. Their average Co_3O_4 particle size is about 11.8 nm, which decreases by 2 nm, compared with that of the Co/Al_2O_3 pellets without any pretreatment. The structure characteristics of the catalysts are listed out in Table 1.

The XRD results shown in Fig. 2 demonstrate that H–β zeolites can only be coated over the Co/Al_2O_3 FTS catalyst pellets that are pretreated with reflux of the hot TEAOH solution (T2 and T3 methods) instead of with the vacuum and ultrasonic pretreatment (T1 method) before the hydrothermal synthesis. Moreover, the color of all these catalysts synthesized as described above was gray, except that of the H–β/Co/Al_2O_3-T3 catalyst which was white.

The external surface SEM image of the H–β/Co/Al_2O_3-T3 catalyst is presented in Fig. 3. The crystallites of the H–β zeolites with a diameter of about 0.2 to 0.5 μm can be clearly observed, evidencing the encapsulation of H–β zeolite coating over the Co/Al_2O_3 pellets after the T3 pretreatment.

The pore size distribution of the catalysts is shown in Fig. 4. One distribution peak is observed with a mean size of 24.7 nm for the Al_2O_3 and Co/Al_2O_3 pellet catalyst, while two distribution peaks, centered at 3.6 and 28.5 nm, appear for the H–β/Co/Al_2O_3-T3 catalysts. The smaller one at 3.6 nm is due to the H–β zeolite coating, as seen in the zoomed area of Fig. 4, and the bigger one at 28.5 nm should belong to the contribution of the structure of Al_2O_3 pellets, which increases about 3.8 nm after the T3 pretreatment and hydrothermal synthesis. The aim of the pretreatment by reflux of hot TEAOH solution is to clean the Co/Al_2O_3 pellets surface and remove the mobile particles through its strong alkali property since the usually utilized NaOH will introduce sodium, which acts as a poisoner for the FTS reaction [30,31], into the catalyst. It also indicates that the Al_2O_3 support can be corroded by the TEAOH solution to soluble species, most likely the $Al(OH)_4^-$, leading to the destruction of the small pores and the enlargement of the pore diameter of the Al_2O_3 pellets. Consequently, a small amount of Co_3O_4 particles supported on the corroded Al_2O_3 supports is also washed away simultaneously.

The detailed properties of the Co/Al_2O_3 pellet catalysts prepared with the T3 pretreatment, followed by drying, are listed out in Table 2. The amount of the H_2 chemisorption uptakes, the reduction degree of Co_3O_4, and the sizes of metallic cobalt particles decrease slightly, while the dispersion of the metallic cobalt increases. It suggests that the larger Co_3O_4 particles are more easily washed away from the Co/Al_2O_3 pellets with the reflux of hot TEAOH solution than the small ones due to the weaker interaction with Al_2O_3 supports than the small Co_3O_4 particles. This also coincides with the XRD results shown in Fig. 2 which indicate that the Co_3O_4 particle size of the H–β/Co/Al_2O_3-T3 catalyst decreases about 2 nm than that of the Co/Al_2O_3 pellet catalysts. Small particles with high dispersion have stronger interaction with Al_2O_3 supports and are more difficultly reduced than the large ones. The differences in the weight of the Co/Al_2O_3 pellet catalyst before and after the T3 pretreatment were estimated, and a mass loss of about 3% was obtained after the T3 pretreatment. Considering that the H_2 chemisorption uptakes slightly decrease about 4% for Co/Al_2O_3-T3 catalyst, which is almost negligible, 7 wt% of cobalt content is still utilized to calculate the cobalt dispersion for the Co/Al_2O_3-T3 catalyst.

Combined with the XRD results shown in Fig. 2, it suggests that both the T2 and T3 pretreatments can increase the number and enhance the strength of the superficial Al–OH groups over the Co/Al_2O_3 pellet due to the strong basicity of TEAOH solution. The Al–OH and Si–OH groups in the zeolite precursor solution reacted easily with these hydroxyls to form stable Al–O–Al and Al–O–Si bonds, and then the framework of the H–β zeolite was anchored on the base of these reticular bonds. After growth with sufficient crystallization time, a H–β zeolite shell was established onto the Co/Al_2O_3 pellets, and a core–shell type encapsulated catalyst, i.e. a H–β zeolite shell-enwrapped Co/Al_2O_3 FTS catalyst, was synthesized.

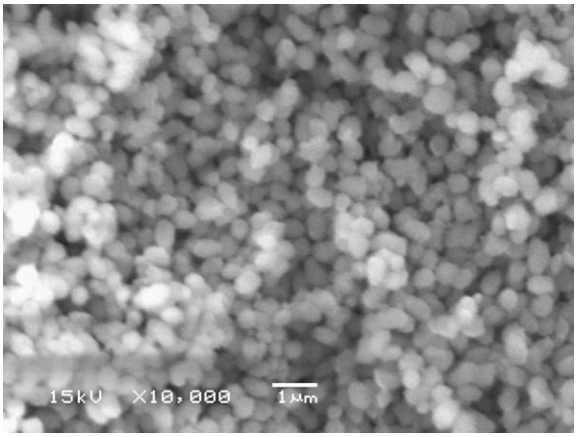

Fig. 3. External surface SEM image of the H–β/Co/Al_2O_3-T3 catalyst.

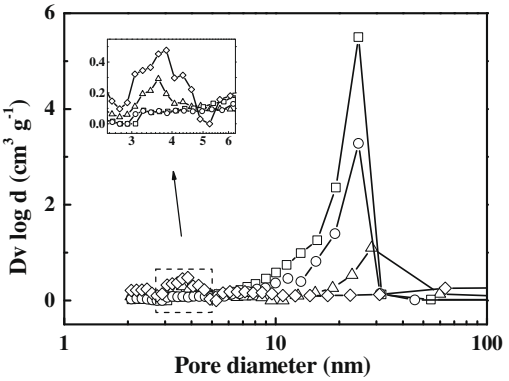

Fig. 4. Pore size distribution of the catalysts: □, Al_2O_3; ○, Co/Al_2O_3; △, H–β/Co/Al_2O_3-T3; and ◇, H–β zeolite.

Table 2
The properties of the Co/Al_2O_3 pellets after the T3 pretreatment.

Catalyst	H_2 uptake (μmol g^{-1})	D_{Co} (%)	Reduction degree (%)	d_{Co} (nm)[a]
Co/Al_2O_3	19.9	5.5	61	17.4
Co/Al_2O_3-T3[b]	19.1	6.1	53	15.7

[a] Co^0 particle size calculated from $d = 96/D\%$.
[b] Drying at 120 °C overnight after the T3 pretreatment, and assuming that the cobalt content is the same as that of the Co/Al_2O_3 catalyst.

After the hydrothermal synthesis, the residual liquid was filtered to remove the deposited solids, and was then evaporated. The finally obtained solid powder was characterized by EDX experiments. As shown in Fig. 5, for the residual solid obtained by evaporation with the T2 pretreatment (Fig. 5A), an element distribution of 0.19% Co, 12.59% Al, and 87.22% Si (molar ratio) is detected. The molar ratio of SiO_2/Al_2O_3 decreases dramatically from the original recipe of 96.53 to 13.9. It suggests that a number of Co and Al species are removed from the Co/Al_2O_3 pellets and are introduced into the synthesis solution during the preparation of the H–β/Co/Al_2O_3-T2 catalyst, leading to the decrease in Si/Al ratio and the appearance of the Co element in the residual powders. However, very interestingly, the EDX result of the residual solid powders obtained with the T3 pretreatment (Fig. 5B) shows that 2.19% Al element and 97.81% Si element are detected without any cobalt element signal, and that the obtained molar ratio, i.e. $SiO_2/Al_2O_3 = 89.3$, is similar to the original ratio, i.e. $SiO_2/Al_2O_3 = 96.53$, of the experimental zeolite precursor solution, as mentioned in the experimental section. It results from the differences in the T2 and T3 pretreatments, which will be discussed later.

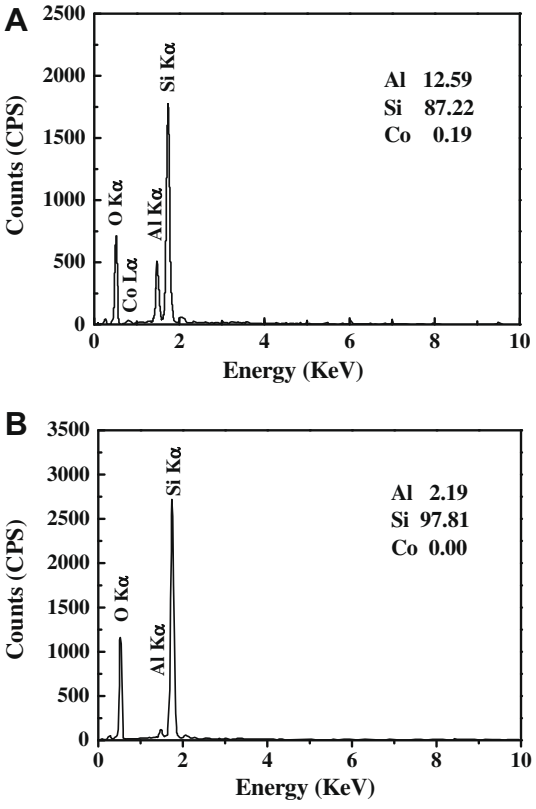

Fig. 5. EDX analysis of the solid obtained from the evaporation of the residual hydrothermal synthesis liquid with different Co/Al_2O_3 pellets pretreatments: (A) T2 method and (B) T3 method.

3.3. The chemical synthesis process of the encapsulated catalysts

The overall surface and cross-sectional SEM images and the radial element distributions of Al, Si, and Co by the SEM–EDX analysis of the encapsulated catalyst prepared with the T2 and T3 pretreatments are compared in Fig. 6. As observed in the SEM images, some cracks existed at the surface of the catalyst prepared with the T2 method (Fig. 6A and E), while the encapsulated catalyst prepared by the T3 pretreatment possessed a perfect H–β coating (Fig. 6B and F). The results of surface EDX analysis indicate that a trace amount of Co element existed on the surface of H–β/Co/Al_2O_3-T2 catalyst (Fig. 6C) with a molar ratio of $SiO_2/Al_2O_3 = 35.2$. Very interestingly, the molar ratio of SiO_2/Al_2O_3 shown in Fig. 6D was 84.2, a value that is similar to the original ratio of zeolite precursor solution (96.53) and that of solid obtained from residual synthesis liquid (89.3) shown in Fig. 5B. Moreover, no Co element was detected at the surface of the H–β zeolite coating prepared with the T3 pretreatment (Fig. 6D). A compact H–β zeolite coating with a thickness of 36 and 16 μm can be clearly observed in the cross-sectional SEM images (Fig. 6E and F) of the H–β/Co/Al_2O_3-T2 and H–β/Co/Al_2O_3-T3 catalysts, respectively. The EDX results (Fig. 6G and H) show that at the interface of the Co/Al_2O_3 substrate and the H–β zeolite coating, the radial distribution of Al element dropped suddenly while that of Si increased, which demonstrates a change from the Co/Al_2O_3 phase to the H–β zeolite phase. However, the Si composition was not zero inside the Co/Al_2O_3 substrate, which indicates that some Si species entered the pores of the Co/Al_2O_3 pellets from liquid phase during the hydrothermal synthesis. Moreover, a small amount of Co component was detected in the H–β zeolite shell (Fig. 6G) of the catalyst that the Co/Al_2O_3 pellets were pretreated only with the hot reflux of the TEAOH solution (T2 pretreatment) while no Co element signal was found in the zeolite coating of the catalyst prepared with the T3 method (Fig. 6H). Considering the fact that the pure H–β zeolite presents a white color, while the Co/Al_2O_3 catalyst pellet is a dark one, these EDX findings can well explain our previous observation that only the catalyst synthesized with the T3 pretreatment on the Co/Al_2O_3 pellets showed a white color, while the others showed a gray one. It resulted from the existence of Co species inside the H–β zeolite shell. The existence of Co species in the H–β zeolite coating will decrease the selectivity of isoparaffins during a FTS reaction since normal paraffins can also be synthesized directly at the surface of the zeolite coating, and then released immediately from the catalyst. Here, we should also notice that only a small amount of Co element was washed away during the TEAOH reflux process since only a trace amount of Co element was detected on the zeolite coating of H–β/Co/Al_2O_3-T2 catalyst (Fig. 6C and G) and the residual solid (Fig. 5A) after evaporation from the hydrothermal synthesis solution, and the H_2 chemisorption uptake of Co/Al_2O_3-T3 pellets was only lowered about 4% than that of the fresh pellet (Table 2).

For the synthesis of the H–β/Co/Al_2O_3-T2 catalyst, the Co/Al_2O_3 pellets were directly added into the hydrothermal precursor solution without any treatment after reflux in the hot TEAOH solution, and, accordingly, the residual $Al(OH)_4^-$ ions and mobile Co_3O_4 particles in the internal pores of the pellets were brought into the hydrothermal synthesis liquid. The leached $Al(OH)_4^-$ ions diffused back toward the outer surface of the pellets and acted as an Al source involved in the H–β zeolite crystallization. This led to the accumulation of Al element at the external surface of the pellets and to the decrease in Si/Al ratio of the zeolite crystal seeds. The accumulation of Al species at the external surface of Co/Al_2O_3 pellets may be beneficial to the growth of the zeolite seeds, and may result in the increase in the thickness of the zeolite coating, which is about 20 μm thicker than that of the H–β/Co/Al_2O_3-T3 catalyst. Meanwhile, the Co_3O_4 particles supported on the corroded Al_2O_3

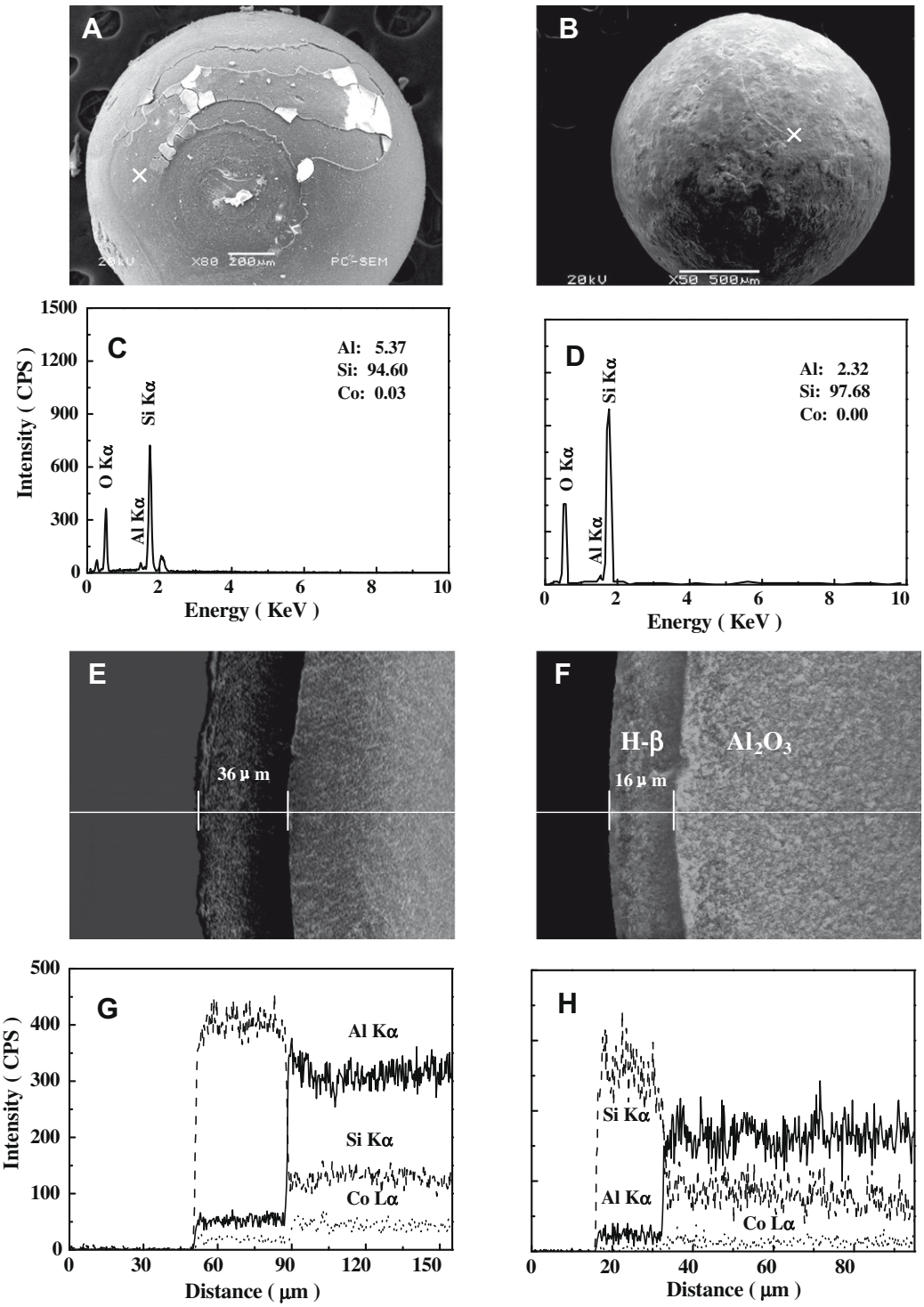

Fig. 6. Overall surface and cross-sectional SEM images and EDX analysis of the H–β/Co/Al_2O_3-T2 catalyst (A, C, E, and G) and the H–β/Co/Al_2O_3-T3 catalyst (B, D, F, and H). The overall surface SEM image: A and B; the surface EDX analysis of the point "x": C and D; the cross-sectional SEM images: E and F; the EDX analysis of the cross-sectional SEM images: G and H.

supports became mobile and accumulated on the external surface of pellets during the hydrothermal synthesis. Moreover, the doped cobalt species in the zeolite coating may hinder the growth of a perfect zeolite coating, and may create cracks and pinholes (Fig. 6A and E), which lead to the gray color of the zeolite shell.

For the synthesis of the H–β/Co/Al_2O_3-T3 catalyst, TEAOH was washed away from the Co/Al_2O_3 pellets with distilled water after reflux of the hot TEAOH solution, and, consequently, EtOH was completely filled into the pores of the Co/Al_2O_3 pellets after 1 day's impregnation, followed by participation in the hydrothermal synthesis precursor solution. The impregnation of EtOH protected the internal pores from the TEAOH corrosion at least at the beginning of hydrothermal synthesis. Therefore, the Si/Al ratio of the zeolite seeds, formed at the beginning of the hydrothermal synthesis stage, remained similar to the ratio of the synthesis liquid. The corrosion of Al_2O_3 supports by TEAOH solution may also happen

Table 3
The catalytic performance of the different catalysts for isoparaffin synthesis directly from syngas.

Catalyst	Zeolite (wt%)	CO conversion (%)	Selectivity (%)		$C_{=}/C_n$ [a]	C_{iso}/C_n [b]	TOF (s^{-1}) [c]		
			CH_4	CO_2			C_n [d]	$C_{=}$	C_{iso}
Co/Al_2O_3	0	88.9	16.1	4.3	0.07	0.02	0.153	0.011	0.003
Co/Al_2O_3-T3[e]	0	85.7	15.9	4.4	0.06	0.01	0.154	0.009	0.001
H–β/Co/Al_2O_3-MX	23.1	83.7	15.2	3.8	0.36	1.91	0.054	0.020	0.084
H–β/Co/Al_2O_3-T3	23.2	81.8	13.3	2.9	0.37	3.13	0.050	0.018	0.097

[a] $C_{=}/C_n$ is the molar ratio of olefin to all normal paraffins with $n > 1$.
[b] C_{iso}/C_n is the molar ratio of all isoparaffins to all normal paraffins with $n > 3$.
[c] Molecule of CO converted per active Co atom per second, which is calculated from the H_2 uptakes of Co/Al_2O_3 for the Co/Al_2O_3 and H–β/Co/Al_2O_3-MX catalysts, and the H_2 chemisorption uptakes of Co/Al_2O_3-T3 for the Co/Al_2O_3-T3 and H–β/Co/Al_2O_3-T3 catalysts.
[d] TOF of normal paraffins is accounted with $n > 1$.
[e] Drying at 120 °C overnight after the T3 pretreatment.

after a prolonged period. However, a thin zeolite coating may already have been formed, and the mobile Co_3O_4, with a mean size of 11.8 nm, cannot move out of the pellets due to the size limitation of the zeolite coating, i.e. 3.6 nm, as observed in Fig. 4. Accordingly, a perfect zeolite coating with white color was obtained with the T3 pretreatment.

All these results demonstrate that zeolite coating is very hard to be constructed onto the Co/Al_2O_3 catalyst pellets without reflux of the hot TEAOH solution (Fig. 2b and c). One function of the hot TEAOH reflux pretreatment was to clean the surface of Co/Al_2O_3 pellets utilizing its strong basicity, and increase the superficial hydroxyl groups over the surface of the pellets, simultaneously, to obtain a pure H–β zeolite shell in the following hydrothermal synthesis. The other function was for TEAOH to act as a corroding reagent to the surface of Co/Al_2O_3 catalyst pellets since a rough surface was much easier to be coated than a polished flat one. Here, NaOH was not utilized since sodium is a well-known poisoner for FTS catalyst [30,31].

3.4. Catalytic test for isoparaffin synthesis

The catalytic performance of the Co/Al_2O_3, Co/Al_2O_3-T3, H–β/Co/Al_2O_3-MX, and H–β/Co/Al_2O_3-T3 catalysts in the direct synthesis of isoparaffins from syngas was investigated, and it is given in Table 3. The products distribution is also shown in Fig. 7. The conventional Co/Al_2O_3 FTS catalyst exhibited a wide product distribution, and normal paraffins were the main products besides a small amount of 1-olefins. Compared with the Co/Al_2O_3 catalyst, the Co/Al_2O_3-T3 catalyst possesses a similar product distribution and shows a slight decrease in the CO conversion from 88.9% to 85.7%, which is due to the loss of cobalt component during the T3 pretreatment, and has been confirmed by H_2 chemical adsorption experiment. For the physical-mixed H–β/Co/Al_2O_3-MX catalyst, isoparaffins were greatly produced, but a small amount of products was still distributed at high carbon numbers, up to C_{24}. Compared with H–β/Co/Al_2O_3-MX catalyst, our encapsulated catalyst presented an excellent isoparaffin selectivity, and the forma-

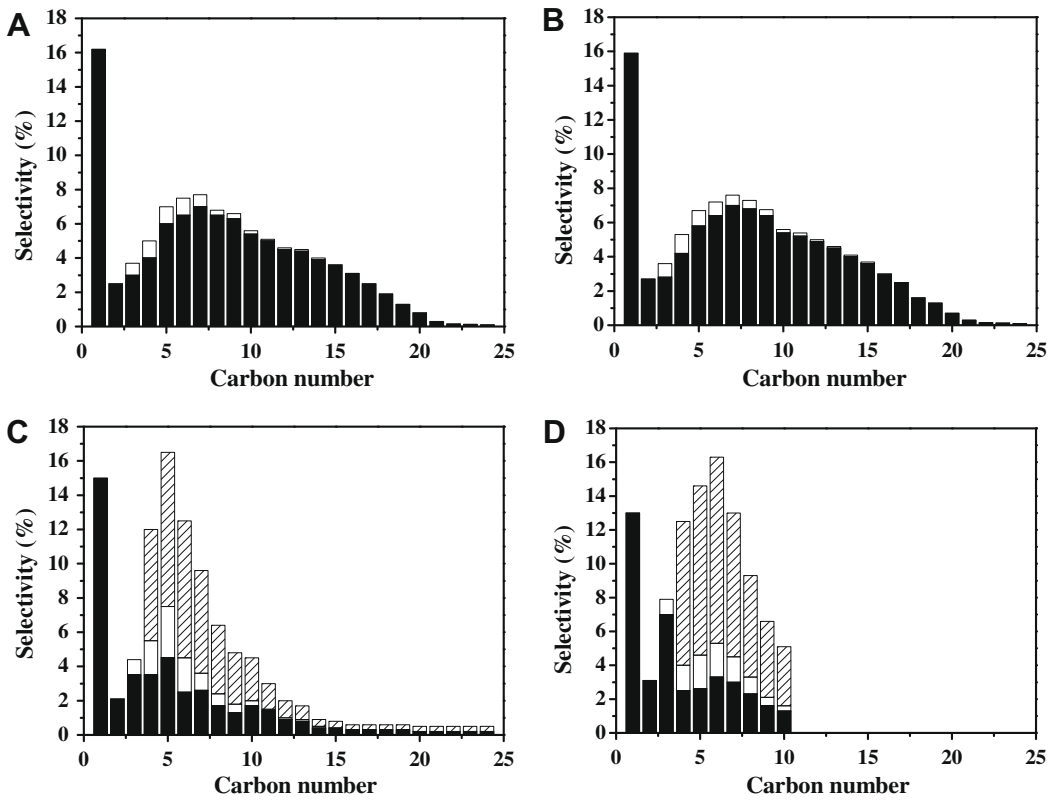

Fig. 7. Products distribution with (A) Co/Al_2O_3 catalyst, (B) Co/Al_2O_3-T3 catalyst, (C) H–β/Co/Al_2O_3-MX catalyst, and (D) H–β/Co/Al_2O_3-T3 catalyst. Blank column: olefin; balck column: normal praraffin; and shadow column: isoparaffin.

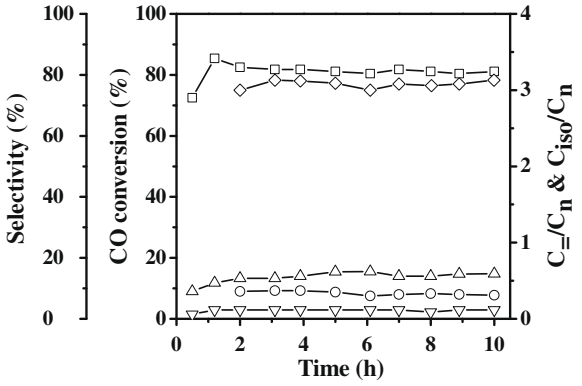

Fig. 8. Time dependence of FTS activity of the H–β/Co/Al_2O_3-T3 catalyst. □, CO conversion; △, CH_4 selectivity; ▽, CO_2 selectivity; ○, $C_{=}/C_n$; and ◇, C_{iso}/C_n.

tion of heavy paraffins (C_{10+}) was completely suppressed. The selectivity of CH_4, CO_2, and normal paraffins ($n > 2$) was of the sequence Co/Al_2O_3 > H–β/Co/Al_2O_3-MX > H–β/Co/Al_2O_3-T3, while the selectivity and turnover frequency (TOF) of isoparaffins were contrary. In particular, the main products were middle isoparaffins (C_4–C_7) for the encapsulated catalyst.

The syngas can pass through H–β zeolite coating to reach the core, i.e. Co/Al_2O_3 FTS catalyst, where synthetic diesel (normal paraffins) is formed, and can then diffuse back the zeolite channel easily with a linear structure. In the H–β zeolite shell, the diffusion rate of hydrocarbons mainly depended on the chain length, and the hydrocarbons, staying longer inside zeolite, with a large carbon number were readily hydrocracked to light hydrocarbons and were isomerized to premier gasoline (isoparaffins) with acidic sites therein [17,21]. Consequently, this led to the highest C_{iso}/C_n ratio, which was improved by 64% compared with that of the physical-mixed catalyst, as well as to the narrow product distribution and a higher TOF for isoparaffin production. Here, we also observed a decrease in CO conversion for the H–β/Co/Al_2O_3-MX and H–β/Co/Al_2O_3-T3 catalysts than for the bare Co/Al_2O_3 catalyst, where FTS wax was directly formed during the FTS reaction. For the H–β/Co/Al_2O_3-MX catalyst, the lower CO conversion may be due to the syngas diffusion being hindered by the physical-mixed micro-porous zeolites around the active cobalt sites. Here, a quantity of FTS wax, formed on Co/Al_2O_3, was simultaneously decomposed by zeolites through hydrocracking and isomerization to promote the proceeding of FTS reaction by dynamic equilibrium. CO diffusion hindrance was probably the major factor than the decomposition of FTS wax. Whereas for our encapsulated catalyst with a core–shell structure, the decrease in CO conversion was not only due to the diffusion hindrance by zeolite coating, but also due to the Co species that were slightly lost during the pretreatment of Co/Al_2O_3 pellets, which led to a little decrease in catalytic active centers. This can be improved by increasing the Co loading on the Al_2O_3 supports.

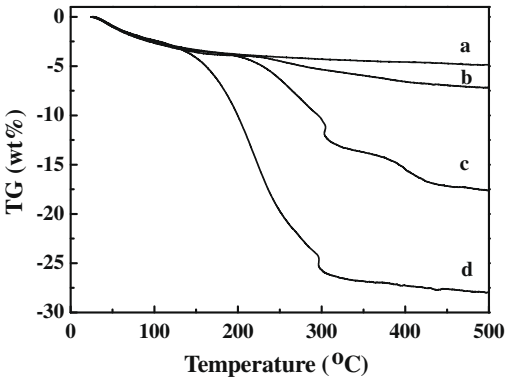

Fig. 9. Differential thermal gravimetric study of the catalysts after 10 h FTS reaction. (a) fresh H–β/Co/Al_2O_3-T3, (b) H–β/Co/Al_2O_3-T3 after 10 h FTS reaction, (c) H–β/Co/Al_2O_3-MX after 10 h FTS reaction, and (d) Co/Al_2O_3 after 10 h FTS reaction.

The time dependence of the FTS catalytic activity with the same reaction conditions is presented in Fig. 8. It shows that the CO conversion is constant at about 81%, and that CH_4 selectivity, CO_2 selectivity, olefin to normal paraffin ratio, and isoparaffin to normal paraffin ratio are also stable without deactivation during the entire experiment. The thermal gravimetry analysis result is shown in Fig. 9 for the fresh and used catalysts. The weight loss below 150 °C is due to the water removal, while that of above 200 °C is ascribed to the coke or the heavy FTS wax combustion. It is clearly observed that the accumulation of coke and heavy FTS wax is serious for conventional Co/Al_2O_3 FTS catalyst (Fig. 9d). After being mixed with H–β zeolite catalyst, the amount of accumulated wax decreases, and the weight loss decreases from 28% to 18%, compared with the Co/Al_2O_3 catalyst. It is due to the hydrocracking and isomerization of the heavy hydrocarbons on the zeolite [17,23]. Whereas for the H–β/Co/Al_2O_3-T3 catalyst, the weight loss is only 7%, a value similar to that for the fresh encapsulated catalyst, i.e. 5%, and the curve is flat. These results coincide with the product distribution results shown in Fig. 7D which indicate that the heavy hydrocarbon C_{10+} is completely suppressed, resulting in little coke or FTS wax accumulation on the encapsulated H–β/Co/Al_2O_3-T3 catalyst.

It should be noted that endothermal hydrocracking reaction can absorb reaction heat of FTS in situ to reduce coke formation, besides converting FTS wax to isoparaffin.

4. Conclusions

By a hydrothermal synthesis method, a novel encapsulated catalyst has been successfully synthesized, that is a H–β zeolite shell was directly coated onto the Co/Al_2O_3 catalyst pellet, forming a core–shell structure. The obtained encapsulated catalyst presented extremely high selectivity and turnover frequency (TOF) for isoparaffins synthesized directly from syngas. Even after 10 h FTS reaction, its catalytic performance was still stable without any deactivation. Moreover, the formation of heavy paraffins (C_{10+}) was completely suppressed, which has also been evidenced by thermal gravimetry analysis that little coke or heavy FTS wax accumulated on the encapsulated catalyst, and the main products were middle isoparaffins (C_4–C_7). This is due to the spatial confinement effect and molecule shape selectivity of the tailor-made encapsulated catalyst.

The pretreatment of the Co/Al_2O_3 catalyst pellets with the hot reflux of the TEAOH solution could clean and corrode the surface of Co/Al_2O_3 pellets, and the superficial hydroxyl groups can also increase on the surface of the pellets, simultaneously. After pretreatment by TEAOH reflux, the internal pore size of the Co/Al_2O_3 pellets was enlarged and some large Co_3O_4 particles were washed away due to the weak interaction with the Al_2O_3 support. Impregnation of Co/Al_2O_3 pellets in EtOH before hydrothermal synthesis is important to protect the internal pores from the TEAOH corrosion, to prevent the cobalt doped into the zeolite coating, and to realize a pure and uniform H–β zeolite coating.

Acknowledgments

The financial aid from NEDO (2005–2007) is greatly appreciated. X. Li thanks the support from Venture Business Laboratory fund of University of Toyama. We also thank our reviewers for helpful suggestions.

References

[1] Y.S. Yan, M.E. Davis, G.R. Gavalas, Ind. Eng. Chem. Res. 34 (1995) 1652.
[2] V. Valtchev, F. Gao, L. Tosheva, New J. Chem. 32 (2008) 1331.
[3] M.A. Zwijnenburg, F. Cora, R.G. Bell, J. Am. Chem. Soc. 133 (2008) 11082.
[4] A. Mitra, T.W. Cao, H.T. Wang, Z.B. Wang, L.M. Huang, S. Li, Z.J. Li, Y.S. Yan, Ind. Eng. Chem. Res. 43 (2004) 2946.
[5] A. McDonnell, D. Beving, A. Wang, W. Chen, Y. Yan, Adv. Funct. Mater. 15 (2005) 336.
[6] H. Wang, L. Huang, B. Holmberg, Y. Yan, Chem. Commun. 16 (2002) 1708.
[7] K. Sato, K. Sugimoto, T. Nakane, Micropor. Mesopor. Mater. 115 (2008) 170.
[8] A. Dong, N. Ren, W. Yang, Y. Wang, Y. Zhang, D. Wang, J. Hu, Z. Gao, Y. Tang, Adv. Funct. Mater. 13 (2003) 943.
[9] N. Ren, Y. Yang, Y. Zhang, R. Wang, Y. Tang, J. Catal. 246 (2007) 215.
[10] X. Peng, M.C. Schlamp, A.V. Kadavanich, A.P. Alivisatos, J. Am. Chem. Soc. 119 (1997) 7019.
[11] V. Valtchev, Chem. Mater. 14 (2002) 956.
[12] A. Dong, Y. Wang, Y. Tang, N. Ren, Y. Zhang, Z. Gao, Chem. Mater. 14 (2002) 3217.
[13] S. Ikeda, S. Ishino, T. Harada, N. Okamoto, T. Sakata, H. Mori, S. Kuwabata, T. Torimoto, M. Matsumura, Angew. Chem., Int. Ed. 45 (2006) 7063.
[14] N. Nishiyama, M. Miyamoto, Y. Egashira, K. Ueyama, Chem. Commun. 18 (2001) 1746.
[15] M. Miyamoto, T. Kamei, N. Nishiyama, Y. Egashira, K. Ueyama, Adv. Mater. 17 (2005) 1985.
[16] H.L. Chum, R.P. Overend, Fuel Process. Technol. 71 (2001) 187.
[17] A. Feller, A. Guzman, I. Zuazo, J.A. Lercher, J. Catal. 224 (2004) 80.
[18] N. Tsubaki, Y. Yoneyama, K. Michiki, K. Fujimoto, Catal. Commun. 4 (2003) 108.
[19] Z. Liu, X. Li, K. Asami, K. Fujimoto, Appl. Catal. A 300 (2006) 162.
[20] Y. Yoneyama, Y. Morii, J. He, N. Tsubaki, Catal. Today 104 (2005) 37.
[21] Y.W. Chen, H.T. Tang, J.G. Goodwin, J. Catal. 83 (1983) 415.
[22] H.H. Nijs, P.A. Jacobs, J. Catal. 66 (1980) 401.
[23] T. Zhao, J. Chang, Y. Yoneyama, N. Tsubaki, Ind. Eng. Chem. Res. 44 (2005) 769.
[24] J. He, Y. Yoneyama, B. Xu, N. Nishiyama, N. Tsubaki, Langmuir 21 (2005) 1699.
[25] J. He, Z. Liu, Y. Yoneyama, N. Nishiyama, N. Tsubaki, Chem. Eur. J. 12 (2006) 8296.
[26] J. Bao, J. He, Y. Zhang, Y. Yoneyama, N. Tsubaki, Angew. Chem., Int. Ed. 47 (2008) 353.
[27] M.V. Landau, L. Vradman, V. Valtchev, J. Lezervant, E. Liubich, M. Talianker, Ind. Eng. Chem. Res. 42 (2003) 2773.
[28] A. Corma, A. Martínez, P.A. Arroyo, J.L.F. Monteiro, E.F. Sousa-Aguiar, Appl. Catal. A 142 (1996) 139.
[29] J. Lee, H. Rhee, Catal. Today 38 (1997) 235.
[30] K.W. Jun, W.J. Shen, K.S. Ramarao, K.W. Lee, Appl. Catal. A 174 (1998) 231.
[31] X. An, B.S. Wu, W.J. Hou, H.J. Wan, Z.C. Tao, T.Z. Li, Z.X. Zhang, H.W. Xiang, Y.W. Li, B.F. Xu, F. Yi, J. Mol. Catal. A: Chem. 263 (2007) 266.
[32] J.M. Zowtiak, C.H. Bartholomew, J. Catal. 83 (1983) 107.
[33] R.C. Reuel, C.H. Bartholomew, J. Catal. 85 (1984) 63.
[34] C.H. Bartholomew, R.J. Farrauto, J. Catal. 45 (1976) 41.